Biological Cybernetics Manuscript-Nr.
(will be inserted by hand later)

Dynamics of the sit-to-stand movement

Patrick D. Roberts and Gin McCollum

R.S. Dow Neurological Sciences Institute,
1120 N.W. 20th Ave, Portland, OR 97209, USA

Received: ¡date¿ / Accepted: ¡date¿

Abstract. The strategies of the sit-to-stand movement are investigated by describing the movement in terms of the topology of an associated phase diagram. Kinematic constraints are applied to describe movement sequences, thus reducing the dimension of the phase space. This dimensional reduction allows us to apply theorems of topological dynamics for two-dimensional systems to arrive at a classification of six possible movement strategies, distinguished by the topology of their corresponding phase portrait. Since movement is treated in terms of topological structure rather than specific trajectories, individual variations are automatically included and the approach is by nature model independent. Pathological movement is investigated, and this method clarifies how subtle abnormalities in movement lead to difficulties in achieving stable stance upon rising from a seated position.

Key words: Sit-to-stand – Movement – Physical therapy – Nonlinear dynamics – Topology

1 Introduction

The most definitive statement that can be made about human movement is that variation is the rule. Not only are there obvious differences in the shapes and sizes of individuals, but everybody has their own unique style of movement as distinctive as their personality. Furthermore, each individual will never repeat exactly the same movement from trial to trial. The myriad of factors that influence these variations are too numerous to control, so we are forced to seek approaches in our study of human movement which are robust under variations of control parameters. In the following, one such approach is developed in which many variations may be captured in a single picture, yet the distinctive differences between various styles and strategies used in the performance of a given task can be determined. In order to take this approach, we must apply techniques used in the study of nonlinear systems. Here it is advantageous to introduce topological concepts into the study of human movement control in order to classify distinct strategy choices that follow from the biomechanics. Once the strategies are determined, it is up to the nervous system to select the appropriate movement for a given situation. In our development of this approach we focus on the sit-to-stand movement for a concrete example, yet it should be understood that the methods developed here may be usefully applied to many movement different studies.

The study of movement has been fraught with difficulties throughout its history. The major reason for this arises from the nature of adaptive biological systems: By controlling variables in experimental investigations, one finds that important components of the functioning system are lost. It seems that one must understand the system as a whole before manipulations can be chosen that get clean results. Yet it is this understanding of the whole system that we strive for in the first place, so we find ourselves trying to pull ourselves along by our boot straps. The situation has led to the development of several different conceptualizations of biological systems and their interaction with their environment.

The most prominent approach in recent years has been a cybernetic metaphor in which the body is treated as a machine which receives sensory inputs and generates motor outputs. Of course, since movement alters the sensory fields, in the language of cybernetics sensorimotor control involves a feedback loop. The "control" task is given to the central nervous system which calculates and adjusts the relevant parameters to accomplish a given task. Differences among research groups arise in the discussion of which parameters are dominant in the control system. Proponents of the *equilibrium point hypothesis* (Asatryan and Feldman 1965) emphasize the endpoints of a movement, where muscle action and mass considerations create a potential well with an equilibrium point that determines the stable final position. Whether this equilibrium position is the parameter controlled by the nervous system, or simply the physical result of some other control mechanism remains difficult to test experimentally.

Correspondence to: Patrick D. Roberts

An alternative approach posits that the nervous system performs *inverse dynamics* – a calculation of the forces needed to accomplish a given task – and then sends the appropriate impulses to the muscles to produce those forces (Hollerbach and Atkeson 1987). This idea is well adapted to the machine model of biological systems, and lends many insights into the study of robotics. A common counter-argument in biological systems is that an inverse dynamical strategy would require too great a calculating load on the nervous system to accurately manipulate a multilinked body with all of the nonlinearities that are involved in motor control.

Increasing the computational load of either of the above proposals are complications arising from the inherent nonlinear couplings between joint torques. Furthermore, physiological studies have shown that there is a complicated relationship between the length of any muscle and the resultant torque on the relevant joints, as well as hysteresis effects from fatigue caused by recent use of the muscles in question and stretching of muscles and tendons. Detailed encoding in the central nervous system of these and other factors would be necessary for the production of accurate large movements. The system may reduce this load by sacrificing accuracy and linearizing much of the calculation (Flanders et al. 1992). The approach of linearization works fine for small movements, but in large movements the contribution of nonlinear component becomes important enough that it would be advantageous to incorporate these elements in the movement strategy itself. Greene (1972) proposed that one needs accuracy only near the endpoints of a movement, where elsewhere in a large movement a "ball park" estimate suffices without involving the fine details of biomechanics in the strategy.

The purpose of this work is to open a means to include the natural, large nonlinearities, and address the issue of the accuracy required to accomplish a large, goal-oriented movement such as rising from a seated position. The sit-to-stand movement is an important movement for patients to master in rehabilitation after stroke or trauma. One can expect that a better understanding of the *physics* of sit-to-stand could have direct therapeutic applications. In spite of the importance of the movement, experimental studies have been comparatively few. One of the reasons for this is the difficulty in establishing experimental paradigms which yield unambiguous results.

Unlike studies of small postural adjustments, investigations of sit-to-stand must contend with the broad individual variations that can be overwhelming in large movements. When correcting for small perturbations about an equilibrium position, such as in small postural adjustment studies, there are really not many choices of postural strategies available. Due to the linear nature of the problem, small variations of a given strategy will not lead to a marked difference in the outcome. In contrast, large movements such as sit-to-stand are essentially nonlinear so that small variations may lead to widely divergent results. We shall see that this also implies that there will be several strategies available to accomplish the same task.

The sit-to-stand studies of Jones, et al. (Jones and Hanson 1961; Jones et al. 1963) have emphasized these individual differences, an aspect which seems to be lost in many of the more recent studies. For instance, in (Jones and Hanson 1961) a significant difference was observed in how far subjects would dip their heads down as they leave the seat. While the head trajectories of some would follow a U-shaped course to build forward momentum in the movement, others would make more use of their arms by swinging them forward to build momentum, and their heads would hardly dip at all. Follow-up studies showed that these individual characteristics remained consistent from trial to trial over the course of several months, emphasizing the individual style of each subject. On the other hand, in studies such as (Kelly et al.1976) it is stated that there are "more similarities than differences" in the motion and EMG patterns for sit-to-stand, yet (Arborelius et al.1992) note widely divergent EMG patterns. One explanation for these differences in results is the difficulty of the study itself as pointed out in (Miller et al. 1989). There is also the fact that different research groups have concentrated on different applications such as chair design (Arborelius et al.1992; Burdett et al. 1985; Fleckenstein et al. 1988; Rodosky et al. 1989; Wheeler et al. 1985), or development of therapy methods (Doorenbosch et al. 1994; Francis et al. 1988; Jeng et al. 1990; Nuzik et al. 1986; Pai and Rogers 1990; Roebreck et al. 1994; Schenkman et al. 1990). The differences in methods and analysis make comparison difficult and results may appear contradictory. We would like to offer some order to this confusion by investigating the nonlinear physics of the movement. We will identify the essential features of sit-to-stand in hopes of encouraging further experimental research.

Another likely reason for disagreement in experimental results is the difficulty in understanding nonlinear behavior itself. By nonlinear we mean here that small differences in the initial conditions can result in large variations of the outcome. Since many aspects of life and the physical world are nonlinear, a deeper understanding of any large movement such as sit-to-stand will help us in approaching other questions of movement in general. In order to approach such potentially complicated problems it is helpful to take a *global* view of the phenomena. As an analogy, one may consider the problem of space flight[1]. Suppose that we want to go to the moon. The straightforward approach is to keep sending up rockets higher and higher and measuring their trajectories. From our modern viewpoint we realize that without a clear understanding of orbital mechanics we will never reach the moon by careful measurements of individual rockets launches. A global understanding is required which views the overall pattern of trajectories that rockets will take in the earth-moon system. An observation relevant to our study is that we can send a rocket to the moon and back even though the multibody problem is unsolvable in closed form. One should not equate nonlinear with non-understandable. The richness of the nonlinear world

[1] We would like to thank Dr. Owen Black for suggesting this example.

leaves many avenues open to explore, and although the information that may be obtained by the methods presented here do not contain the precision of closed form solutions, nonetheless this information illuminates the range of movement options. It is in this spirit that we approach the problem of human movement.

Our purpose is to show how to link the biomechanics of movement to topological aspects of dynamics. This approach may therefore be termed *topological biomechanics*. The goal is to determine the possible movement strategies rather than compute the exact joint torques necessary for a specific movement. Approximate equations of motion are used as a starting point to identify fixed points in the phase space from which one may determine a set of topologically distinct pictures of the dynamics in the phase space. We then find different styles and strategies of sit-to-stand which fit these pictures. The classification of movement in terms of topologically distinct pictures allows for broad individual variations, yet can distinguish healthy movements from pathological, at least pathological in the sense of difficulty in accomplishing the task of rising from a chair to stable stance. In the next section we introduce our description of movement in terms of a constrained Hamiltonian system. The derived equations of motion form merely a starting point for further analysis using geometric methods of topological dynamics. Section 3 contains our main results, in which the essential topological structure of the equations of motion from Section 2 is used to classify the structurally stable phase portraits of the sit-to-stand movement. The necessary theorems and methods of topological dynamics are introduced. The section with examples of sit-to-stand movement strategies which correspond to our classification. We conclude in Section 4 with a discussion of the advantages and limitations of this approach, and address potential applications to physical therapy and rehabilitation.

2 Description of movement

In order to form a broad base to describe movement we will include not only the kinematics, but the dynamics as well. Since there is some ambiguity in the usage of these terms, we define *kinematics* as the purely geometric aspects of the movement, while *dynamics* include the momenta and forces involved in the movement. Considering the dynamics extends the parameter space from purely spatial coordinates to include the momenta. The reason for doing this is twofold: Momentum is important for the sit-to-stand movement since there may be phases of the movement that are statically unstable. Secondly, a phase space description allows one to take advantage of theorems from the study of nonlinear dynamics, thus resting the analysis upon well established foundations.

The natural approach to describing a mechanical system in terms of position and momentum variables is to derive Hamilton's equations of motion. Since Hamiltonian systems are conservative by definition, it may be argued that this application is rather unrealistic in the context of driven and damped biological systems. However, the Hamiltonian approach forms a good starting point from which we may develop a general framework because dissipative systems can be regarded as perturbations of Hamiltonian systems (Guckenheimer and Holmes 1983). Since the aim is not to construct a specific *model* of the sit-to-stand movement, but investigate the *pattern* of the movement, Hamiltonian system are useful to yield a "saddle point" between structurally stable regions in the space of dynamical systems. Instead of modeling the specific action of specific muscles, we assume that the action of the neuromuscular system establishes functional relationships between joint angles which appear in our equations in the form of kinematic *constraints*. Here we do not attempt to answer questions as to how these constraints are implemented, whether by preset habits and reflexes, or through sensorimotor feedback. It might be added that upon establishing the family of constraints necessary to accomplish a specific task, the underlying neurophysiology may then be probed by observing changes in the constraints due to perturbations of environmental factors or neurological deficit.

2.1 Constrained Hamiltonian dynamics

> Imposing constraints on a system is simply another method of stating that there are forces present in the problem that cannot be specified directly but are known rather in terms of their effect on the motion of the system.
> H. Goldstein, *Classical Mechanics* (1980)

In order to apply constraints to a dynamical system, there are several approaches that we may take. If we are interested in the constraint *forces* we may use Lagrange multiplier techniques (but see (Arnold 1989, p. 96) for ambiguities associated with this). Dirac has developed a method for applying constraints to Hamiltonian systems (Dirac 1950) which may be used for more complicated constraints than those we investigate here. A straightforward approach is taken here by simply eliminating variables at the onset and then derive Hamiltonian's equations of motion in terms of the remaining degrees of freedom.

The starting point will be an inverted double pendulum (Hemami and Jaswa 1978; McCollum and Leen 1989) in which the first link is extendable (see Fig. 1). The canonical variables can easily be derived from the Lagrangian of the system after the constraints are applied even though the form of the variable may be quite non-trivial. The Lagrangian for the system may be written as (Marsden and Scheurle 1993)

$$L(\mathbf{q}_1,\mathbf{q}_2,\dot{\mathbf{q}}_1,\dot{\mathbf{q}}_2) = \frac{m_1}{2}|\dot{\mathbf{q}}_1|^2 + \frac{m_2}{2}|\dot{\mathbf{q}}_1+\dot{\mathbf{q}}_2|^2 - m_1 g \mathbf{q}_1\cdot\hat{\mathbf{y}} - m_2 g(\mathbf{q}_1+\mathbf{q}_2)\cdot\hat{\mathbf{y}}, \tag{1}$$

where $\mathbf{q}_1$ and $\mathbf{q}_2$ are vectors describing the pendulum links, $\hat{\mathbf{y}}$ is the vertical Cartesian basis vector, and $\dot{\mathbf{q}}_1 = d/dt(\mathbf{q}_1)$. We convert to polar coordinates in the sagittal plane using the relations:

Figure 1. Definitions of variables. The vectors $\mathbf{q}_1$ and $\mathbf{q}_2$ define the positions of the masses m_1 and m_2 of the double pendulum,and m_2 sits at the center of mass of the trunk. The length ℓ is constant and r is variable. The Cartesian basis vectors are $\hat{\mathbf{x}}$ and $\hat{\mathbf{y}}$. The angles of the segments with respect to the vertical are given by θ_1 and θ_2.

$$\begin{aligned}\mathbf{q}_1 &= r\sin(\theta_1)\hat{\mathbf{x}} + r\cos(\theta_1)\hat{\mathbf{y}}\\ \mathbf{q}_2 &= \ell\sin(\theta_2)\hat{\mathbf{x}} + \ell\cos(\theta_2)\hat{\mathbf{y}},\end{aligned} \tag{2}$$

where ℓ is a constant. In these variables the Lagrangian takes the form,

$$\begin{aligned}&L(r,\theta_1,\theta_2,\dot{r},\dot{\theta}_1,\dot{\theta}_1) =\\ &\frac{1}{2}(m_1+m_2)(\dot{r}^2+r^2\dot{\theta}_1^2)+\frac{1}{2}m_2\ell^2\dot{\theta}_2^2\\ &+m_2(\dot{r}\ell\dot{\theta}_2\sin(\theta_1-\theta_2))+r\ell\dot{\theta}_1\dot{\theta}_2\cos(\theta_1-\theta_2)\\ &-(m_1+m_2)gr\cos\theta_1 - m_2g\ell\cos\theta_2.\end{aligned} \tag{3}$$

At this point one could define the conjugate momenta corresponding to the above configuration variables, construct the Hamiltonian, and derive Hamilton's equations of motion, but this would tell little about the sit-to-stand problem. The above Lagrangian corresponds to nothing more than a free massless rod in a gravitational field with masses m_1 and m_2 attached to either end. In order to describe a sit-to-stand movement we must constrain the variables. In our choice of coordinates, r and θ_1 are related to the ankle and knee angles and the dimensions of the leg. Although the center of mass of the leg is not located at the hip joint, this approximation makes a good starting point for our purposes for reasons to be addressed in the next section. The trunk angle to vertical is given by θ_2, and ℓ is determined by the center of mass of the body above the hip.

In describing the sit-to-stand, the movement can be divided into only two phases: before and after lift-off (though other schemes are possible (Schenkman et al. 1990)). Before lift-off forward momentum can be generated by throwing the trunk forward and perhaps utilizing the arms. Whatever movement occurs only determines the lift-off momentum. After lift-off the knees extend and both θ_1 and θ_2 approach zero. The functional relationship between these variables will be written in the form of kinematic constraints to describe the movement after lift-off. Since in our coordinates "forward momentum" will translate into angular momentum about θ_1 in the sit-to-stand range, we will leave this variable free. Three examples of the relation between constraint equations and whole body movements are given in Fig. 2. It should be noted here that these examples where chosen because the yield different topologies in their respective phase plots. More generally, the kinematic constraints are represented by functions of θ_1,

$$\begin{aligned}r &= f_r(\theta_1)\\ \theta_2 &= f_2(\theta_1).\end{aligned} \tag{4}$$

Note that each of these constraints takes out two degrees of freedom in the Lagrangian since

$$\begin{aligned}\dot{r} &= \dot{\theta}_1 f_r'(\theta_1)\\ \dot{\theta}_2 &= \dot{\theta}_1 f_2'(\theta_1),\end{aligned} \tag{5}$$

where $f'(x) = d/dx\, f(x)$. In Fig. 2 *natural units* of body mass and height are used such that the mass and height of the individual are normalized to one; $m_1 + m_2 = 1$ and $\ell + f_r(\theta_1 = 0) = 1$. In the following, the proportions used in the calculations are: $\ell = 1/3$ of the distance from the floor to the center of the upper segment's center of mass when $\theta_1 = 0$, $m_1 = 1/4$, and $m_2 = 3/4$ (McCollum and Leen 1989). The first movement sequence (Fig. 2A) is the strategy that most people use when rising from a firm chair of moderate height. The second is designed to approximate a physical therapy technique use to help people with neurological deficits to stand up independently. The objective is to position the center of mass at least over the ankles or somewhat forward so that the subject is already statically stable at the onset of the movement, and stable stance is then achieved by extending the knees. The third example looks much like the first, but we have added a small oscillation to the trunk angle constraint. This is to simulate the typical hip wobble observed in patients with cerebellar injury, and though this wobble is hardly noticeable in the figure, we will later see that the effect on the dynamics can be quite strong.

Now the relations in equations (4) and (5) can be used to eliminate r, θ_2, $\dot{r}$, and $\dot{\theta}_2$ and derive the constrained equations of motion. The Lagrangian now reads

$$L(\theta_1,\dot{\theta}_1) = \tag{6}$$

$$\frac{1}{2}F(\theta_1)\dot{\theta}_1^2 - m_2g(mf_r(\theta_1)\cos(\theta_1)+\ell\cos(f_2(\theta_1))), \tag{7}$$

where

$$\begin{aligned}F(\theta_1) = {}& mm_2\left(f_r'(\theta_1)^2+f_r(\theta_1)^2\right)+\ell^2 f_2'(\theta_1)^2\\ &+2\ell f_2'(\theta_1)\left(f_r'(\theta_1)\sin(\varphi(\theta_1))+f_r(\theta_1)\cos(\varphi(\theta_1))\right),\end{aligned}$$

and we have defined the variables

$$m = (m_1+m_2)/m_2, \text{ and } \varphi(\theta_1) = \theta_1 - f_2(\theta_1). \tag{8}$$

Now we may work towards the equations of motion by first computing the conjugate momentum:

Figure 2. Examples of constraint functions: In all of these examples: $f_r(\theta_1) = 7/12 + 1/12 \tanh(4\theta_1 + 2)$. (A) Momentum method: $f_2(\theta_1) = 1/4 - 1/4 \tanh(4\theta_1 + 2)$. (B) Noes over toes: $f_2(\theta_1) = 1/2 - 1.2 \tanh(4\theta_1 + 2)$. (C) Hip wobble: $f_2(\theta_1) = 1/4 - 1/4 \tanh(4\theta_1 + 2) + .1 \sin(8\theta_1)$.

$$p_1 = \frac{\partial L}{\partial \dot{\theta}_1} = F(\theta_1)\dot{\theta}_1. \tag{9}$$

The function $F(\theta_1)$ serves as an effective mass on a simple pendulum with the effective potential composed of the last two terms of equation (3);

$$V_{eff}(\theta_1) = m_2 g(m f_r(\theta_1)\cos\theta_1 + \ell \cos(f_2(\theta_1)). \tag{10}$$

Taking the Legendre transformation,

$$H(\theta_1, p_1) = p_1\dot{\theta}_1 - L(\theta_1, \dot{\theta}_1), \tag{11}$$

one obtains the Hamiltonian:

$$H(\theta_1, p_1) = \frac{p_1^2}{2F(\theta_1)} + V_{eff}(\theta_1). \tag{12}$$

It is now straightforward to derive Hamilton's equations of motion;

$$\dot{\theta}_1 = \frac{\partial H}{\partial p_1} = \frac{p_1}{F(\theta_1)}$$
$$\dot{p}_1 = -\frac{\partial H}{\partial \theta_1} = G(\theta_1)p_1^2 - V'_{eff}(\theta_1), \tag{13}$$

where

$$G(\theta_1) = \frac{F'(\theta_1)}{2F(\theta_1)^2}. \tag{14}$$

2.2 Stable stance

The above equations of motion can be used to describe rising from a chair if the appropriate constraints are inserted, but they contain no mechanism for maintaining stable stance. On the contrary, they have an unstable fixed point, a saddle point at $\theta_1 = 0$. By making alterations in these equations near the saddle point, we may construct a means for achieving stable stance. The simplest manipulation is to add an extra term to the potential function which will generate a restoring force to hold the inverted pendulum upright. To study standing posture we will, for the remainder of this section, fix: $r = constant$ so that $\dot{r} = 0$ and $f'_r(\theta_1) = 0$.

The unaltered potential is given in Fig. 3A along with its derivative function which is the resultant force. The associated phase diagram shown in Fig. 3B shows the unstable saddle point. It is desirable to add a "dimple" in the potential near the $\theta_1 = 0$ to insure stable stance. This can be accomplished by adding a simple Gaussian term of the form

$$V_s(\theta_1) = -ae^{-b\theta_{cm}^2}, \ 0 < a < 1, \ 0 < b \tag{15}$$

such that a suitable choice of parameters a and b we arrive at the potential depicted in Fig. 3C. It should be stressed here that the exact functional form of the potential is unimportant here as long as there is a stable point near $\theta_1 = 0$. Define $\theta_{cm} = \theta_{cm}(r, \theta_1, \theta_2)$ to be the angle from the pivot point on the floor to the center of mass of the double pendulum which must be near zero for unsupported stance. This perturbs the system in a way which preserves the Hamiltonian form so that it is still a conservative system. Note that in the phase plane diagram (Fig. 3D) there is now a *center* at the origin and oscillatory motion about this point in the neighborhood of the origin. The choice of the stabilizing mechanism will be made explicit by the form of the constraint function $f_2(\theta_1)$ which constrains the hip angle to the ankle angle; for example, it could represent a hip or an ankle synergy (Nashner and McCollum 1985). The simplest form is a linear relation such as

$$\theta_2 = f_2(\theta_1) = \kappa\theta_1 \tag{16}$$

Figure 3. Potential functions and the corresponding phase portraits. (A) The solid line is the potential function and the dotted line shows the force induced by this potential. (B) In the phase plot corresponding to (A), $(\dot{\theta}_1, \dot{p}_1)$ follow the arrows and at the origin the potential levels off so that we have a fixed point. Since the forces on either side of this fixed point push away from it, the trajectories split and we have a saddle point. (C) And extra term is added giving the potential a dimple at $\theta_1 = 0$. (D) In this phase plot corresponding to (C), there are now three fixed points, and the one at the origin has restoring forces on either side so that there are oscillations.

so that the a rotation about the ankle, with the hip moving in the same direction is given by $\kappa > 0$ and counter-rotating hip and ankle angles by $\kappa < 0$. The net result for either of the strategies is to give a net torque to the ankle joint which arises from the $V_s(\theta_1)$ term.

The perturbation which leads from Fig. 3B to 3D is an example of a perturbation which changes the *topological* form of the phase diagram by the deformation from Fig. 3B to 3D. At present suffice it to say that by topology we mean the connectivity of the phase flows. The phase plane is naturally separated into several regions in the area of interest to the problem at hand $(-\pi/3 < \theta_1 < \pi/3)$. Fig. 3B is divided into four regions by the separatrix centered at the single saddle point at $\theta_1 = 0$, but the perturbation $V_s'(\theta_1)$ splits the saddle point into two saddle points, connected by paths which circle a fifth region about the origin. In the unperturbed case, trajectories with small positive momenta at $\theta_1 = 0$ have forward flows which diverge away from their backwards flows. After the perturbation, such trajectories soon return upon themselves. In the next section we will identify different topologies of phase portraits in order to classify the different strategies of rising from a seated position.

3 Topological dynamics

The importance of including the many individual variations in a description of large movements was discussed in the introduction. For instance, the masses of the body segments are explicit in the equations of motion above. Although the natural units are chosen such that the total mass is unity for each individual, the proportions between the masses of the segments will vary and affect the form of the phase plot. Other effects will arise from varying proportions of lengths of the segments and variations in the constraints which describe each individual movement pattern. As stated in the last section, the inertial ellipsoid of the lower limb has been approximated by setting the mass at the joint. The true position of the center of mass of the leg is another variation that we wish to include into our methods. Having chosen a phase diagram approach, the inclusion of individual variations is deeply entwined with the concept of *structural stability*: A phase portrait is structurally stable if the topological form does not change under small perturbations, such as variations in the exact position of the center of mass of each segment. We will now investigate the possibilities for structural stability which are available given a wide class of two-dimensional phase diagrams.

Figure 4. Elementary Fixed points: (A) Sink, (B) Source, (C) Saddle point, (D) Attractor node, (E) Repellor node.

Figure 5. Limit cycles generated by equation (17). (A) $\epsilon > 0$, $\delta < 0$; (B) $\epsilon < 0$, $\delta > 0$.

3.1 Exercises in constrained variability

It is important make clear the distinction between *structural* stability and the kind of stability associated with a limit set, *i.e.* a region on a phase portrait where no trajectory flows out from the region's boundary. This latter case can be called *neutral* or *Liapounov* stability, depending upon whether the trajectories return upon themselves or terminate at a fixed point. The kinds of two-dimensional limit sets that exist are summed up by the Poincaré-Bendixon theorem (Abraham and Marsden 1985):

Theorem 1 (Poincaré-Bendixon). *For vector fields on compact, orientable, two-dimensional manifolds, limit sets must be either limit cycles, limit points, or limit tori.*

We will not encounter limit tori in the following and refer the reader to (Abraham and Marsden 1985) for further information.

Examples of limit cycles and limit points can be obtained from the following equations:

$$\begin{aligned} \dot{\theta}_1 &= p_1 \\ \dot{p}_1 &= \sigma\theta_1 + \epsilon p_1 + \delta p_1^3, \end{aligned} \tag{17}$$

where $\sigma = \pm 1$, ϵ, and δ are real numbers. The form of these equations has been chosen so that they contain much of the behavior that we are investigating. The fixed points are found where $\dot{\theta}_1 = \dot{p}_1 = 0$: the point where all motion stops. If we let $\sigma = -1$ and $\delta = 0$, then the phase plot of equation (17) will have at the origin a *sink*, *source*, or *center* depending upon whether $\epsilon > 0$, $\epsilon < 0$, or $\epsilon = 0$. The center was encountered at the origin of Fig. 3D, and the sink and source are shown in Fig. 4. The reason that the center is not included in Fig. 4 is that it is not structurally stable under certain non-Hamiltonian perturbations, because the center stands at the *bifurcation point* of the topological change in the phase plot where the fixed point goes from a sink to a source, or *vice-versa*. On the other hand, if we choose $\delta \neq 0$, so that ϵ has the opposite sign of δ, we have the possibility that the system will be driven in some regions of the phase plane while damped in others. This situation would yield the limit cycles shown in Fig. 5. Finally, if ϵ and δ are nonzero and of the same sign, then we recover the source or sink of Fig. 4.

Another possibility for equation (17) is to allow $\sigma = +1$. In this case we find a saddle point at the origin which we have seen before in Fig. 3B. Saddle points are examples of unstable fixed points. The fixed points portrayed in Fig. 4 constitute the full set of *elementary* fixed points in two dimensions. All of the elementary fixed points are structurally stable under perturbations, but only the two sinks yield stable attractor sets.

In order to list structurally stable phase diagrams associated with any large movements we have yet to state the global rules for structurally stable connections between the fixed points. In two dimensions these rules are easily provided by Peixoto's Theorem (Peixoto 1961) which states:

Theorem 2 (Peixoto). *A smooth vector field on a two-dimensional compact manifold is structurally stable if and only if;*
1. The limit sets consist only of fixed points and periodic orbits (limit cycles).
2. The number of fixed points and closed orbits is finite and each is elementary.
3. There are no connections between saddle points.
Furthermore, if the manifold is orientable, structurally stable flows are generic in the space of all two-dimensional flows.

By knowing the relationship between the equations of motion and the corresponding phase flows, this theorem can be a very powerful tool in constructing structurally stable descriptions of dynamics. Not only do these three above conditions insure structurally stable flows, but the theorem tells us that such flows are typical. This means that in the space of all phase flows, those which are structurally stable form a dense set. Thus, in the sit-to-stand

Figure 6. Compactification the the cylinder for the application of the Poincaré-Bendixon theorem. The cylinder is truncated and coordinate patches are fused to the ends in a smooth manner so that the vector field may be extended over the entire surface.

example, for an individual's given size and mass distribution, there is a vanishing probability that the choice of constraints on any given trial will yield a phase flow which is *not* structurally stable.

There is an obvious problem with the application of Peixoto's theorem as stated above to the sit-to-stand movement. The theorem is proven for a vector field on a *compact* manifold, whereas the manifold defined by the variables θ_1 and p_1 is a cylinder which is unbounded in the $\pm p_1$ directions. Of course, we are only interested in a region of relatively small momenta and with θ_1 limited to the range; $-\pi/3 < \theta_1 < \pi/3$. However, the theorem does not directly apply to such a bounded region: we will have vector flows tangent to the boundary for which a small perturbation can be found to change the flow so that it passes outward through the boundary and back (see e.g. (Arrowsmith and Place 1990)), thus changing the topology at the boundary. Although we may choose a region such that these boundary effects are unimportant to our problem, in order to keep a well defined concept of structural stability, it is more convenient to map the base manifold to a compact surface. This can be accomplished by truncating the cylinder sufficiently far from the θ_1-axis and defining coordinate patches as end caps which smoothly close the p_1-coordinate as in Fig. 6. The base manifold will then have the topology of a sphere which is a compact, orientable manifold so the theorem applies.

3.2 Applications to sit-to-stand

The equations of motion that we derived using Hamiltonian methods serve as a framework to which physically motivated perturbations may be applied to yield structurally stable phase diagrams. The "skeleton" of the phase portrait is the number and approximate location of the fixed points on the compactified cylinder of Fig. 6. Without linear perturbations, the equations of motion (13), in combination with the additional potential term of equation (15) yield a center at $\theta_1 = 0$ and $\theta_1 = \pi$, and two saddle points on either side of $\theta_1 = 0$ as depicted in Fig. 3D. The compactification procedure will also yield a center at each of the poles. We now alter this basic structure by perturbing the equations of motion with approximate terms to achieve a structurally stable phase flow. Figure 3D is clearly not structurally stable because there are trajectories that connect the saddle points, and the fixed point at the origin is not elementary. This can be made into a structurally stable system by adding a linear term as was done in equation (17). Since we are investigating a situation which involves stable stance, a sink at $\theta_1 = 0$ is appropriate as in Fig. 7. This is justified by assuming that energy can be taken out of the system such as by an ankle torque or a shear force with the floor from a hip synergy. The damping may be restricted to the region about the origin by giving the extra term the form, $-cp_1 \exp(-d\theta_1^2)$, with a suitable choice of $c, d > 0$. A similar damping term may be added in the neighborhood of $\theta_1 = \pi$ and

Figure 7. Perturbations of the system given in eq.(17) by a term, ϵp_1, in the second equation, and with $\delta = 0$. (A) $\epsilon = 0$, (B) $\epsilon < 0$, (C) $\epsilon > 0$. Note that (B) and (C) are structurally stable, but only (B) has a stable attractor set.

Figure 8. Perturbations of the system given in eq.(18). (A) $\delta = 0$ and $g(\theta_1) = 1$, (B) $\delta < 0$, or $g(\theta_1)$ is larger for negative θ_1 than positive, (C) $\delta > 0$, or $g(\theta_1)$ is larger for positive θ_1 than negative. Note that none of these phase portraits are structurally stable.

at the poles of the compact cylinder so that these centers are converted to elementary fixed points. Since the region of physical interest to the sit-to-stand movement is far from these fixed points, it is unimportant which elementary fixed point is chosen, as long as it insures the overall structural stability as given by Peixoto's theorem. The diagram can be "fleshed-out" by including the trajectories from the saddle points such that there are no saddle connections. This procedure yields a discrete set of phase portraits on the compact cylinder, which by Peixoto's theorem are the generic flows that follow from perturbations of Hamilton's equations, in eq.(13). It can now be understood how

the requirement of structural stability automatically includes many variations. By stating that there is a postural adjustment strategy to maintain stable stance means that any variation in the size or mass of the individual, or strength of the postural adjustment will not remove the stable region about the origin. One must consider that when taking this approach we lose any exact detail of individual trajectories, but we are seeking general principles which can be drawn from the overall geometry of the phase diagrams.

Before listing the possible phase portraits, it is useful to address the issue of what effect the individual constraints will have. The constraints enter the equations of

motion (13) through the two functions $F(\theta_1)$ and $G(\theta_1)$ and the potential function. In order to demonstrate how they affect the relevant region of the phase diagrams, we may without loss of generality investigate the following system of equations:

$$\begin{aligned}\dot{\theta_1} &= g(\theta_1)p_1 \\ \dot{p_1} &= a\theta_1^3 - b\theta_1 + \alpha p_1^2,\end{aligned} \tag{18}$$

For a suitable choice of a and b, and setting $g(\theta_1) = 1$ and $\alpha = 0$, the phase portrait for this system of equations is topologically equivalent to Fig. 3D in the region shown, therefore they correspond to the same topological structure as our equations derived from the Hamiltonian, eq.(13). If we allow $g(\theta_1)$ to vary, we find that trajectories speed-up in the θ_1 direction as $g(\theta_1)$ becomes greater. This means that if the value of $g(\theta_1)$ is greater for θ_1 near the right saddle point than for the left, then the trajectory originating from the left saddle point will overshoot the other saddle point. Thus, we find the bifurcation behavior as shown in Fig. 8 for $g(\theta_1 < 0) < g(\theta_1 > 0)$, and the other bifurcation occurs when this asymmetry is reversed.

In order to understand the effect of the αp_1^2 term we consider the slope of the trajectory at $\theta_1 = 0$. By inspection, if $\alpha > 0$, then the slope for $p_1 > 0$ is positive so that, as before, the trajectory leading from the left saddle point will overshoot the right. Likewise, for $\alpha < 0$, the slope will be negative over the origin and the trajectory reconnects with the left saddle point. Referring to equation (13), we see that the effect of the constraints through the functions $F(\theta_1)$ and $G(\theta_1)$ can be summed up in this simple bifurcation diagram (Fig. 8). The only other influence of the constraints will be in their effect on the form of the potential function.

Another important variable in our discussion is the boundary of the region which contains the sit-to-stand movement. Although we have constructed the phase space on a compact cylinder, we are mostly interested in forward movement, *i.e.* where $p_1 \geq 0$. In addition, the choice of lift-off angle for θ_1 will be related to the position of the feet relative to the rest of the body. After determining the structurally stable phase flows on the compact cylinder, one must then impose a boundary onto the surface in order to select the relevant area for the sit-to-stand movement. Upon determining the constraints for a movement, the lift-off angle falls into a range of values which are physically possible considering requirements of chair design and body proportions.

In Fig. 9 we present the main result of this paper: the phase diagrams which may arise from the above geometric considerations. Limit cycles have been excluded for simplicity and because they would not aid much in our understanding of the problem at hand. The positive flows follow from positive momenta at lift-off. These are all structurally stable phase diagrams which follow from perturbations of Hamilton's equations of motion given in equation (13). A distinction is made between whether the left-most saddle point is at an angle which is greater or less than the lift-off angle because this parameter may change the number of distinct outcomes of the phase flows. Now that we have a classification of possible phase diagrams from the principles of topological dynamics, we next investigate various movement strategies to find which diagram may be associated with which set of constraints.

It is useful here to consider one of these phase plots as an example in the context of the sit-to-stand movement. If we allow the left hand boundary of Fig. 9B to be the lift-off angle, then the initial momentum at lift-off is represented by the height above the θ_1 axis. For small momenta, the trajectories increase in θ_1, but then reverse; representing the subject falling back into the seat. As we increase the momentum, we will eventually cross the trajectory terminating at the first saddle point. Here begins a finite region where all trajectories lead to the sink at the origin so that the subject obtains stable stance. The upper boundary of this attractor region is marked by the trajectory terminating at the second saddle point. At momenta above this trajectory, the subject will fall forward to the floor, assuming that no effort is made to correct for this overshot.

3.3 Examples of sit-to-stand movements

We are now in the position to examine in detail the three examples of sit-to-stand strategies in Fig. 2, and match them to their corresponding phase plane topologies in Fig. 9. These examples were chosen not only because they are of clinical interest, but also because they expose the three factors involved in determining the phase topology from the constraint equations. Recalling Hamilton's equations (13) for the constrained double pendulum, we see that the constraints enter in three terms: as a factor $1/F(\theta_1)$ in the first equation, as the factor $G(\theta_1)$ in the second equation, and in the potential term. In the previous subsection we investigated the effect of the first two of these on the topology of the phase portrait, but now we must consider that $G(\theta_1)$ is related to $1/F(\theta_1)$ by minus the derivative with respect to θ_1. This is important when considering the combined effects of these terms: When the value of $1/F(\theta_1)$ is greater for negative θ_1 than positive θ_1, the trajectories tend to close on the right, but this may also imply that the slope of $1/F(\theta_1)$ is negative near the origin so that $G(\theta_1)$ takes on a positive value which tends to close the trajectories on the left. We can see how this competition of factors is resolved in our first example.

Corresponding to the momentum method shown in Fig. 2A, we graph the form of $1/F(\theta_1)$ and $G(\theta_1)$ in Fig. 10A. Clearly $1/F(\theta_1)$ is significantly greater to the left of and far enough from the origin so that the influence would be to yield the topology of Fig. 9A or 9B. Had this function been symmetric about $\theta_1 = 0$, then the influence of $G(\theta_1)$ would be to cancel the effect of $1/F(\theta_1)$, but due to the asymmetry, $G(\theta_1)$ is small enough near the origin that it is $1/F(\theta_1)$ that dominates. Finally, it must be noted that for the $f_2(\theta_1)$ constraint, the movement of the upper torso does not affect the potential enough to alter the topology.

Figure 9. The 6 structurally stable phase diagrams following from perturbations of equation (13), excluding limit cycles. Lift-off momenta lie along the left boundary, and solid trajectories terminate at saddle points.

In the second example (Fig. 2B), the dominating effect comes from the potential function. Although the functions shown in Fig. 10B are quite similar to 10A, the extreme forward bow of the trunk moves the center of mass over the pivot point on the floor throughout the duration of the movement. This is in the realm of topologies given in the right column of Fig. 9. We may eliminate 9F since the form of $F(\theta_1)$ is so similar to the first example.

It is in the third example that the power of this approach becomes evident. This is shown in Fig. 2C where we have added to the first example a small hip wobble. Although the difference between these two examples is not obvious from viewing the stick figures, the corresponding graph in Fig. 10C makes the difference all too clear. Indeed, it is difficult to see which of the two functions will dominate, but note that the right-left asymmetry of $1/F(\theta_1)$ is washed out by the wobble, and $G(\theta_1)$ gives enough influence to yield the topology depicted in Fig. 9C. If this represented a patient with a brain injury, one can now see by the dynamics how such a hip wobble would hinder attempts to rise from a seated position. Using a method such as this may help to identify movement dysfunction from subtle abnormalities such as the hip wobble in this example.

4 Discussion

In this work we have developed a description of large body movement, in particular, the sit-to-stand movement, which makes the nonlinear nature of the movement explicit and allows for individual variations. To summarize, we have described movement in terms of the following sequence: Reflexes and learned habits relevant to a given task determine the kinematic constraints which in turn determine the geometry of the associated phase portrait. Finally, movements and actions arise out of this geometry as the final parameters are chosen, such as the forward momentum at lift-off in the sit-to-stand examples given above. We emphasize that this sequence should not be considered as some preset motor program, but an ongoing sensorimotor integration in which the entire sensorimotor system is active in determining the constraints and what choices to make in the resultant geometry. One may ponder whether the central nervous

Figure 10. Relavant functions for the three examples of sit-to-stand strategies shown in figure 2. Solid line; $G(\theta_1)$, and dashed line; $1/F(\theta_1)$. Note that here (A) and (C) are easily distinguished.

system uses a method of constraint functions in order to coordinate movements and navigate in the environment. By maintaining certain distance and angle relations, an organism could greatly reduce the number of degrees of freedom in motor behavior. It is hoped that such a formulation of the problems of motor control will prove useful in experimental design to help determine more specific details of the sensorimotor system, such as testing the limitations of the motor control proposals given in the introduction.

With the generality of our approach we have, of course, sacrificed the details of the movement. Since we concentrate on the global topology of the whole relevant phase plane, we lose the predictability of following a specific trajectory of a particular model given a set of initial conditions. We argue that there is a need to obtain an overall, global viewpoint to help us understand movement, yet there are applications where specific descriptions of forces and trajectories become necessary. The design of prosthetics, for instance, would require a more detailed description of movement than our final result given here, as would applications in the field of robotics. Detailed modeling can be helpful even in theoretical approaches to human movement, such as when testing certain optimization assumptions. However, these phase portraits should prove useful for some applications just as they are. For example, a physical therapist might recognize which phase portrait applies to a particular patient, or would be a desired goal for therapy. A physical therapist could also distinguish movements described by the different regions of each phase portrait.

It should prove interesting to explore the possibility of generalizations on the kinematic constraints presented above. Although the constraints were chosen to give us autonomous equations of motion (independent of time), one might find a need to include time delays in the constraint functions. Such constraints would more accurately describe the distal to proximal sequence of joint actions seen in postural adjustment studies than the simple "equal-time" constraints given in section 2.2. Here we have not been concerned with the details of the postural adjustment strategy, as long as one exists; however, in other movement strategies, such temporal sequencing might display some interesting nonlinearities that would otherwise be missed. One might also find it more useful to describe a movement by constraining the momentum components as opposed to the purely kinematic constraints given here. With such constraints one must be careful to insure that the dynamical constraints are consistent, and in such a case the methods developed by Dirac are most applicable (Dirac 1950).

In spite of these limitations, we feel that this approach can shed light on not only the sensorimotor system in general, but on certain therapeutic applications as well. By making nonlinear effects in movement explicit, we are given hints as to what to look for in movement disorders, and what steps may be taken in order to improve the patient's quality of life. As stated earlier, the third example in Section 3.3 has much in common with the kinematic results following damage to the cerebellum. By first determining what problems may exist for the successful completion of a task by looking at the topological dynamics, we can then ask ourselves what kinematic constraints would contribute to the problems. Then we need only find a means of correcting the kinematics constraints through physical therapy or perhaps mechanical support in order to aid in the improvement of motor skills. In the example given here, an improved ability to rise from a chair can add greatly to a patient's self-sufficiency and independence.

Acknowledgement. We wish to thank Jan Holly for discussions and many helpful suggestions on the manuscript. This research was supported by National Institutes of Health grants RO1-NS23209 and RO1-DC02482.

References

1. Abraham RH, Marsden JE (1985) Foundations of Mechanics, 2nd ed., Reading, MA: Benjamin/Cummings.
2. Arborelius UP, Wretenberg P, Lindberg F (1992) The effects of armrests and high seat heaghts on lower-limb joint load and muscular activity during sitting and rising. Ergonomics **35**, 1377-1391.
3. Arnold VI (1989) Mathematical Methods of Classical Mechanics, 2nd ed., Berlin Heidelberg New York: Springer.
4. Arrowsmith DK, Place CM (1990) An Introduction to Dynamical Systems, Cambridge: Cambridge University Press.
5. Asatryan DB, Feldman AG (1965) Functional tuning of the nervous system with control of movement or maintenance of a steady posture. Biofizika **2**, 925-935.

6. Burdett RG, Habasevich R, Pisciotta J, Simon SR (1985) Biomechanical comparison of rising from two types of chair. Phys. Ther. **65**, 1177-1183.
7. Dirac PAM (1950) On generalized Hamiltonian dynamics. Can. J. Math. **2**, 129-148.
8. Doorenbosch CAM, Harlaar J, Roebreck ME, Lankhorst J (1994) Two strategies of transferring from sit-to-stand; The activation of monoarticular and biarticular muscles. J. Biomechanics **27**(11) 1299-1307.
9. Flanders M, Helms Tillery SI, Soechting JF (1992) Early stages in a sensorimotor transformation. Beh. Brain Sci. **15**, 309-362.
10. Fleckenstein SJ, Kirby RL, MacLeod DA (1988) Effect of limited knee-flexion range on peak hip movements of force while transferring from sitting to standing. J. Biomech. **21**, 915-918.
11. Francis ED, VanSant AF, Newton RA (1988) Variability in the sit-to-stand motion in children and aldults: a developemental hypothesis. Phys. Ther. **68**, 866 Abstract.
12. Greene PH (1972) Problems of organizing motor systems. Prog. Theor. Biology **2**, 303-338.
13. Guckenheimer J, Holmes P (1983) Nonlinear Oscillations, Dynamical Systems, and Bifurcations of Vector Fields, Berlin Heidelberg New York: Springer.
14. Hemami H, Jaswa VC (1978) On the three-link model of the dynamics of standing up and sitting down. IEEE Trans. **SMC-8**, 115-120.
15. Hollerbach JM, Atkeson CG (1987) Deducing planning variables from experimental arm trajectories: Pitfalls and possibilities. Bio. Cyb. **56**, 279-292.
16. Jeng S-F, Schenkman M, Riley PO, Lin S-J (1990) Reliability of a clinical kinematic assessment of the sit-to-stand movement. Phys. Ther. **70**, 511-520.
17. Jones FP, Hanson JA (1961) Time-Space pattern in a gross body movement. Perception and Motor Skills **12**, 35-41.
18. Jones FP, Hanson JA, Miller JF, Bosson J (1963) Quantitative analysis of abnormal movement: the sit-to-stand pattern. Am. J. Phys. Med. **42** 208-218.
19. Kelly DL, Dainis A, Wood GK (1976) Mechanics and muscular dynamics of rising from a seated position. In: Komi PV: Biomechanics V-B. pp. 127-134 Baltimore, MD: University Park Press.
20. Marsden JE, Scheurle J (1993) Lagrangian reduction and the double pendulum. Z. angew. Math. Phys. **44** 17-43.
21. McCollum G, Leen TK (1989) Form and exploration of mechanical stability limits in erect stance. J. Motor Behavior **21**, 225-244.
22. Miller M, Schultz A, Alexander N, Warwick D, Ashton-Miller J (1989) Dynamics of rising from a chair: expermental data collection. Symp. on Biomech., ASME Annual Meeting, 329-332.
23. Nashner LM, McCollum G (1985) The organization of human postural movements: A formal basis and experimental synthesis, Beh. Brain Sci. **8**, 135-172.
24. Nuzik S, Lamb R, VanSant A, Hirt S (1986) Sit-to-stand movement pattern: a kinematic study. Phys. Ther. **66**, 1708-1713.
25. Pai Y-C, Rogers MW (1990) Control of body mass transfer as a function of speed of ascent in sit-to-stand. Med. Sci. Sport & Ex. **22**, 378-384.
26. Peixoto M (1961) Structural stability on two-dimensional manifolds, Topology **2**, 101-121.
27. Rodosky MW, Andriacchi TP, Andersson GBJ (1989) The influence of chair height on lower limb mechanics during rising. J. Ortho. Res. **7**, 266-271.
28. Roebreck ME, Doorenbosch CAM, Harlaar J, Jacobs R, Lankhorst J (1994) Biomechanics and muscular activity during sit-to-stand transfer. Clin. Biomech. **9**(4) 236-244.
29. Schenkman M, Berger RA, Riley PO, Mann RW, Hodge WA (1990) Whole-body movements during rising to standing from sitting. Phys. Ther. **70**, 638-651.
30. Wheeler J, Woodward C, Ucovich RL, Perry J, Walker JM (1985) Rising from a chair: influence of age and chair design. Phys. Ther. **65**, 22-26.

This article was processed by the author using the LaTeX style file *cljour2* from Springer-Verlag.

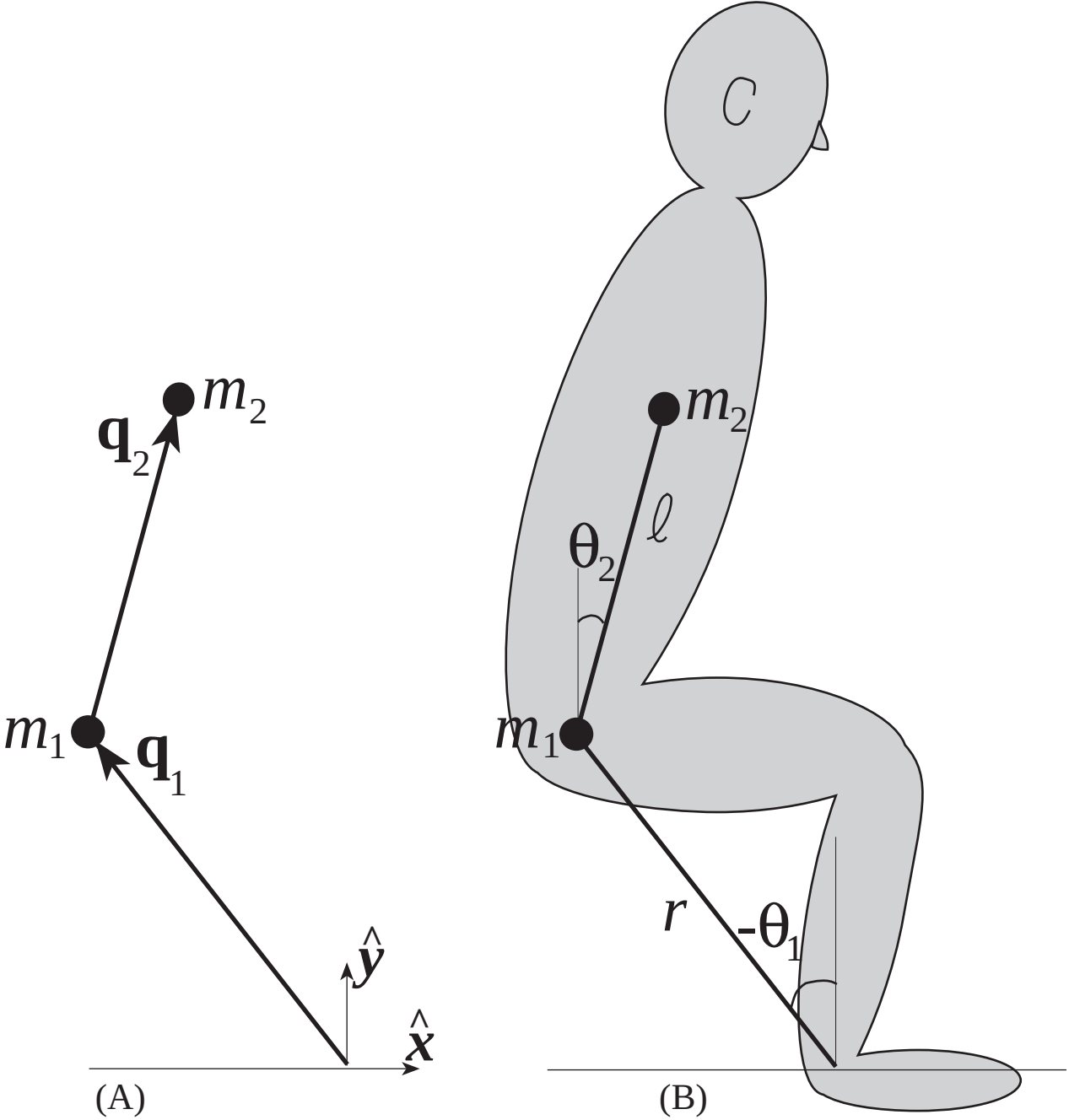
m_2
$\mathbf{q}_2$
m_1
$\mathbf{q}_1$
$\hat{y}$
$\hat{x}$
(A)
C
m_2
ℓ
θ_2
m_1
r
$-\theta_1$
(B)

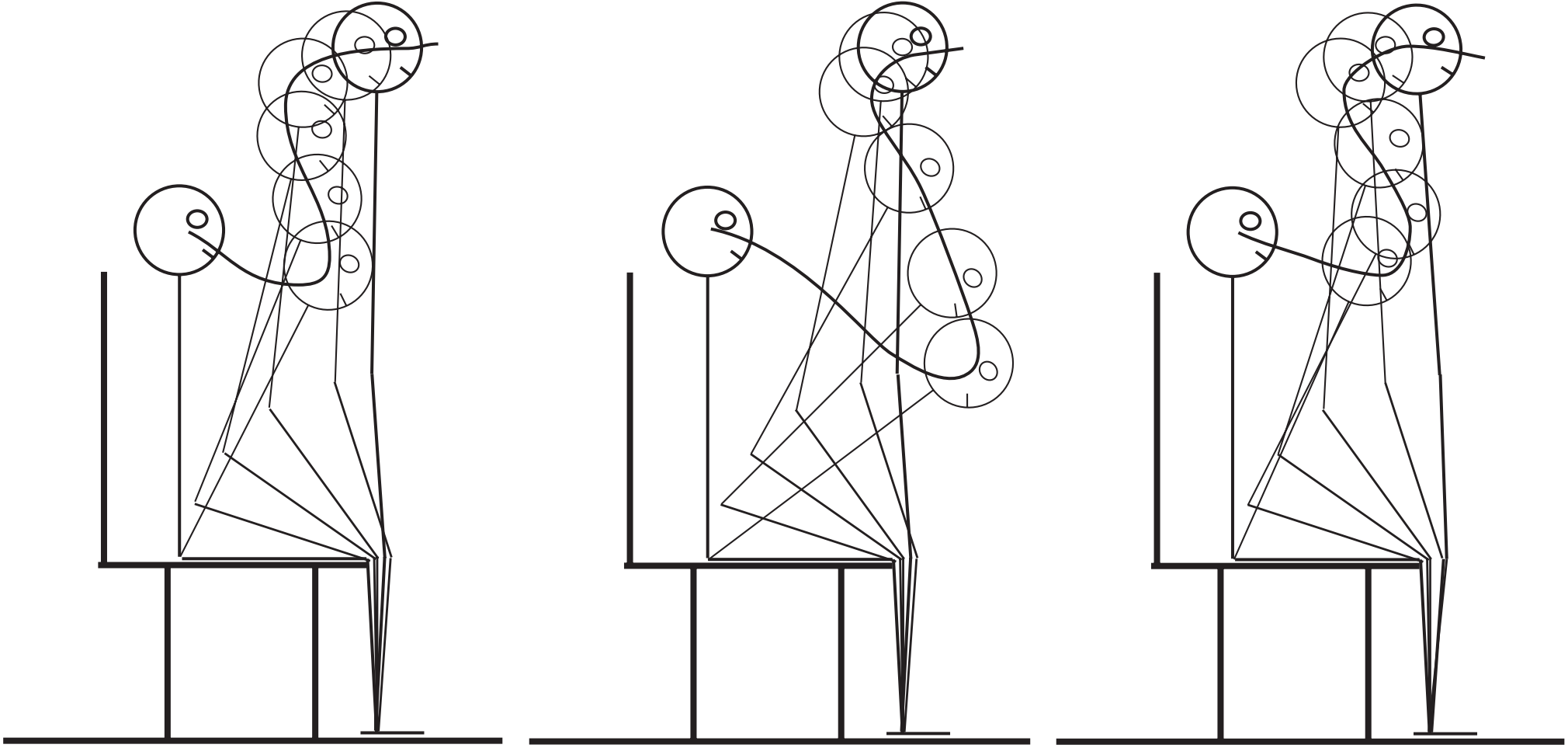
(A)
(B)
(C)

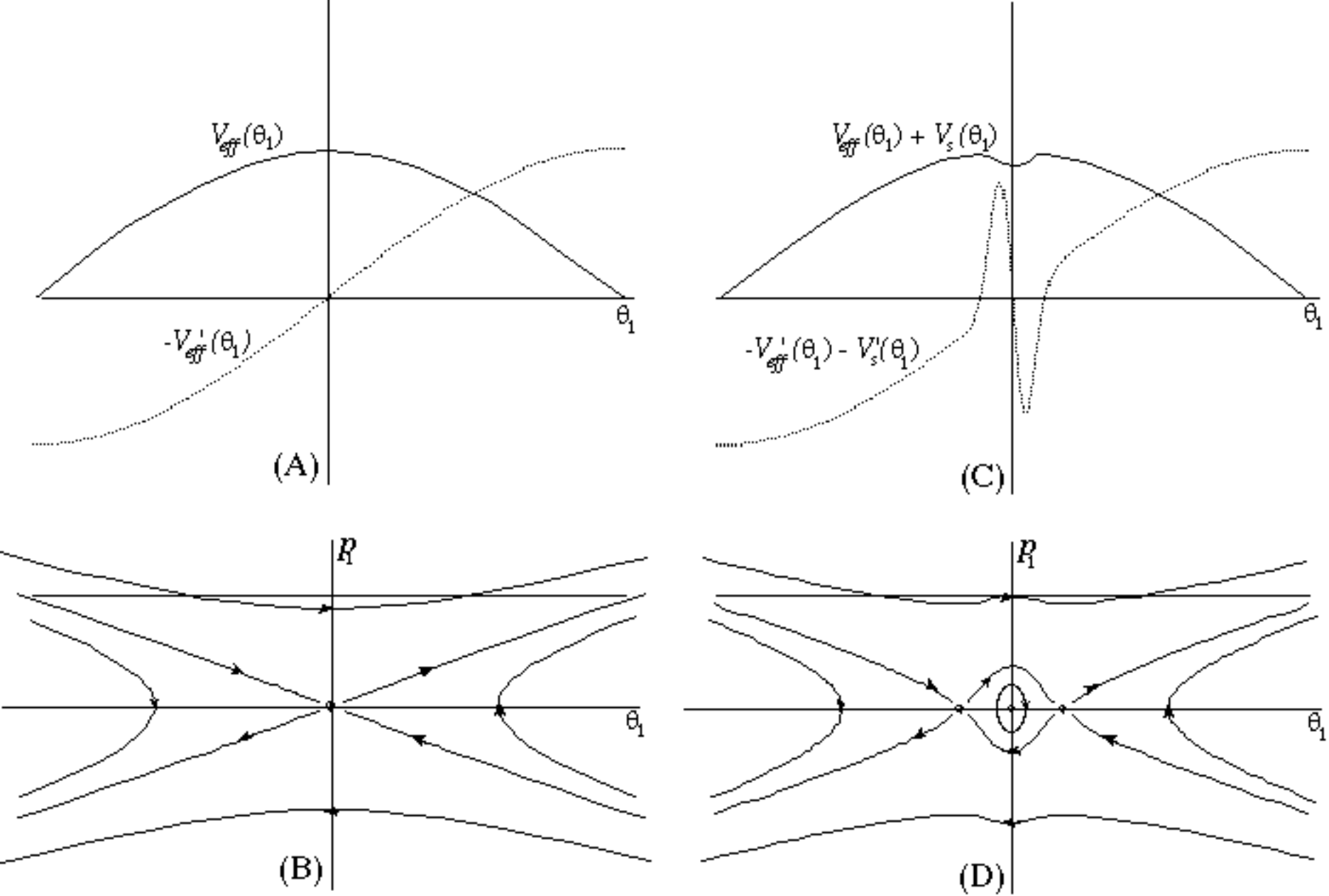
$V_{eff}(\theta_1)$
θ_1
$-V'_{eff}(\theta_1)$
(A)
$V_{eff}(\theta_1) + V_s(\theta_1)$
θ_1
$-V'_{eff}(\theta_1) - V'_s(\theta_1)$
(C)
P_1
θ_1
(B)
P_1
θ_1
(D)

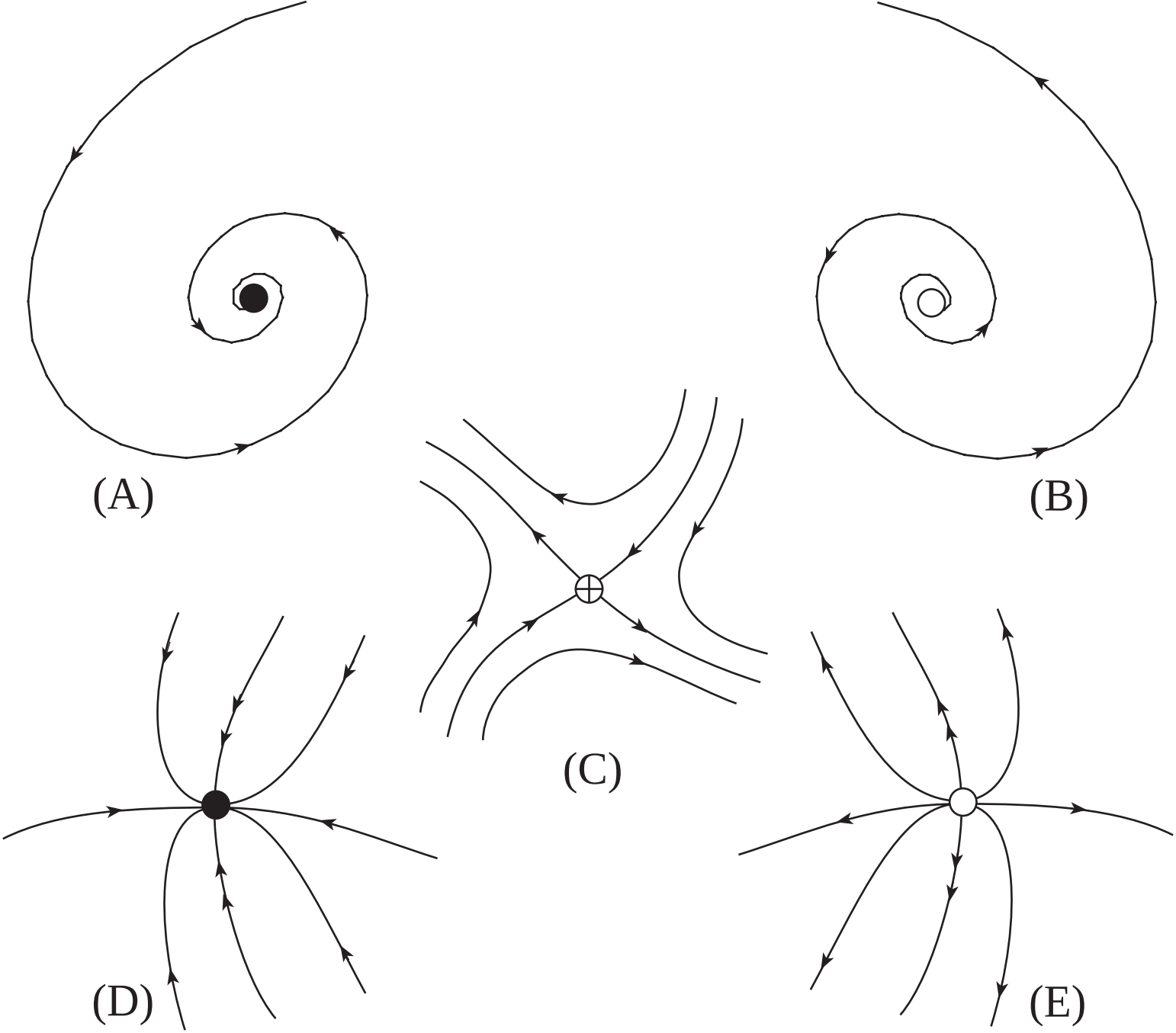
(A)
(B)
(C)
(D)
(E)

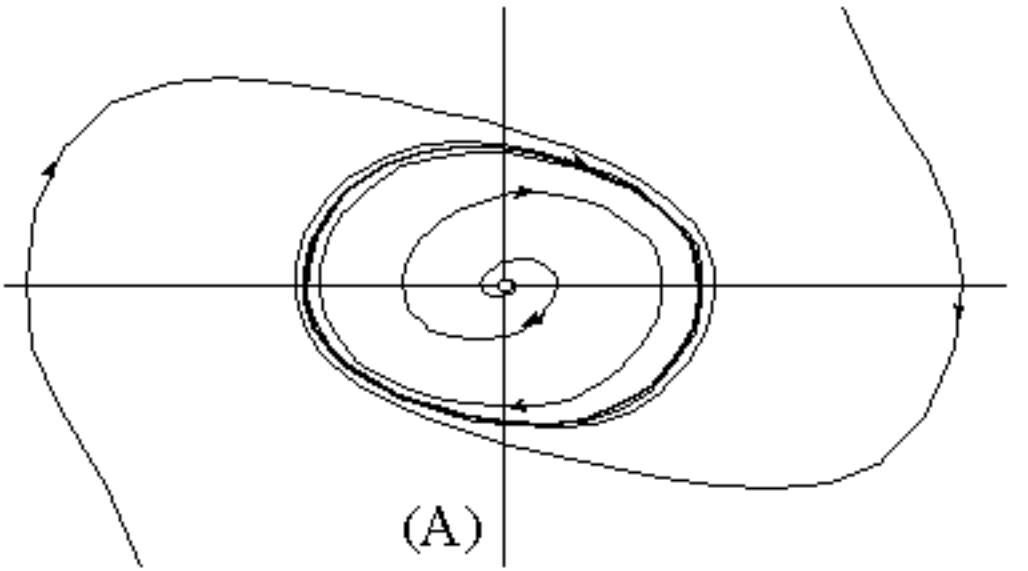
(A)

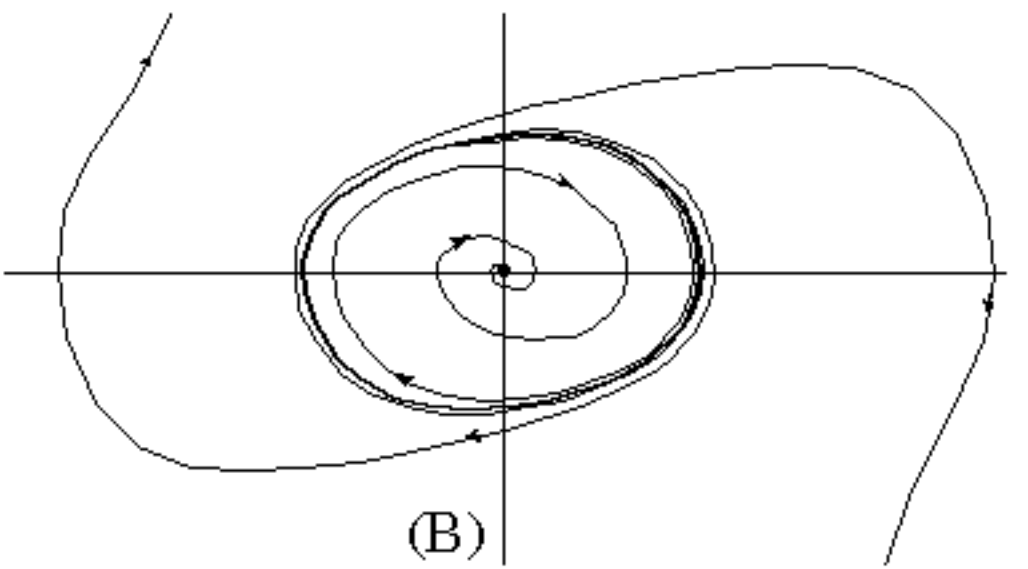
(B)

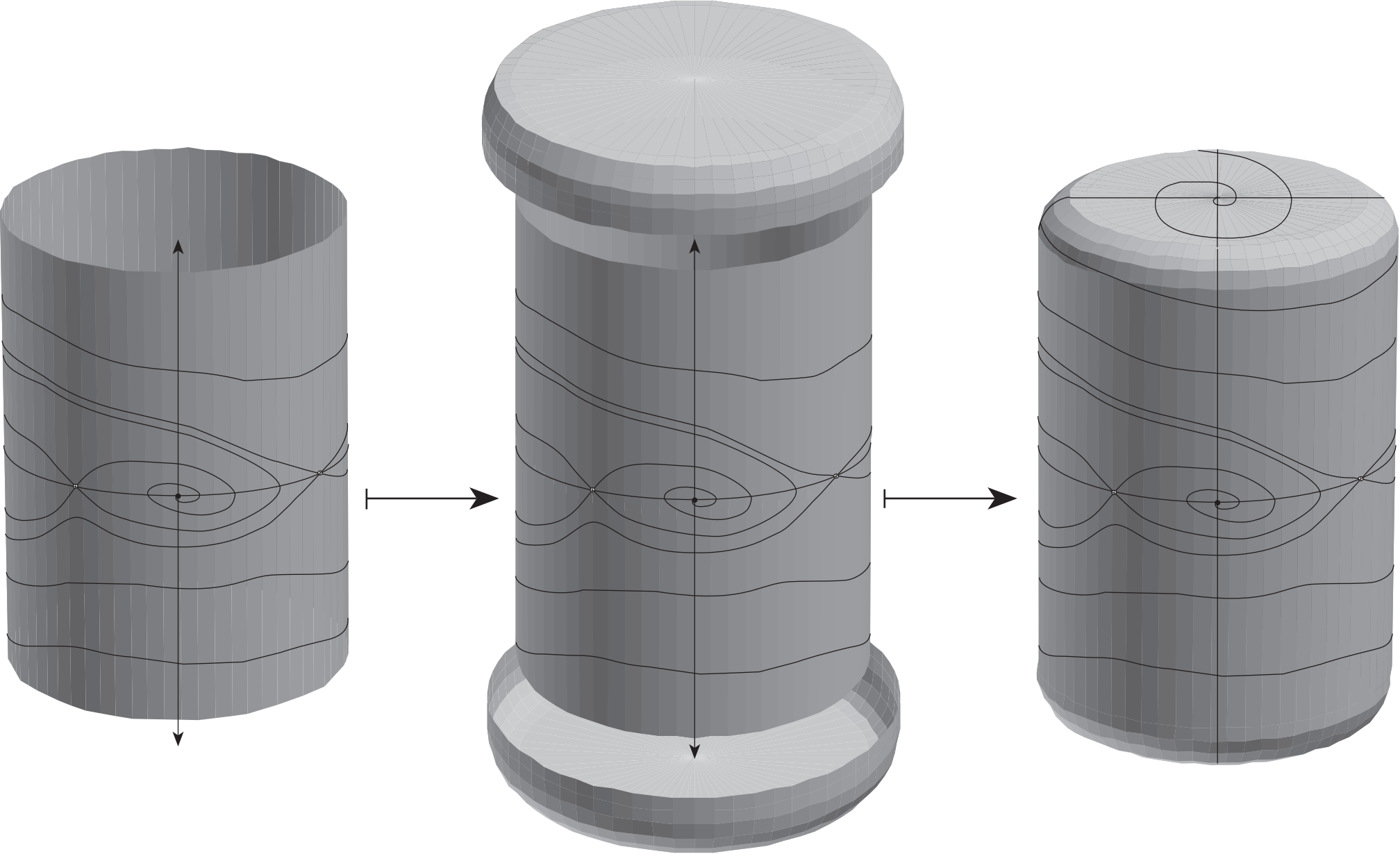

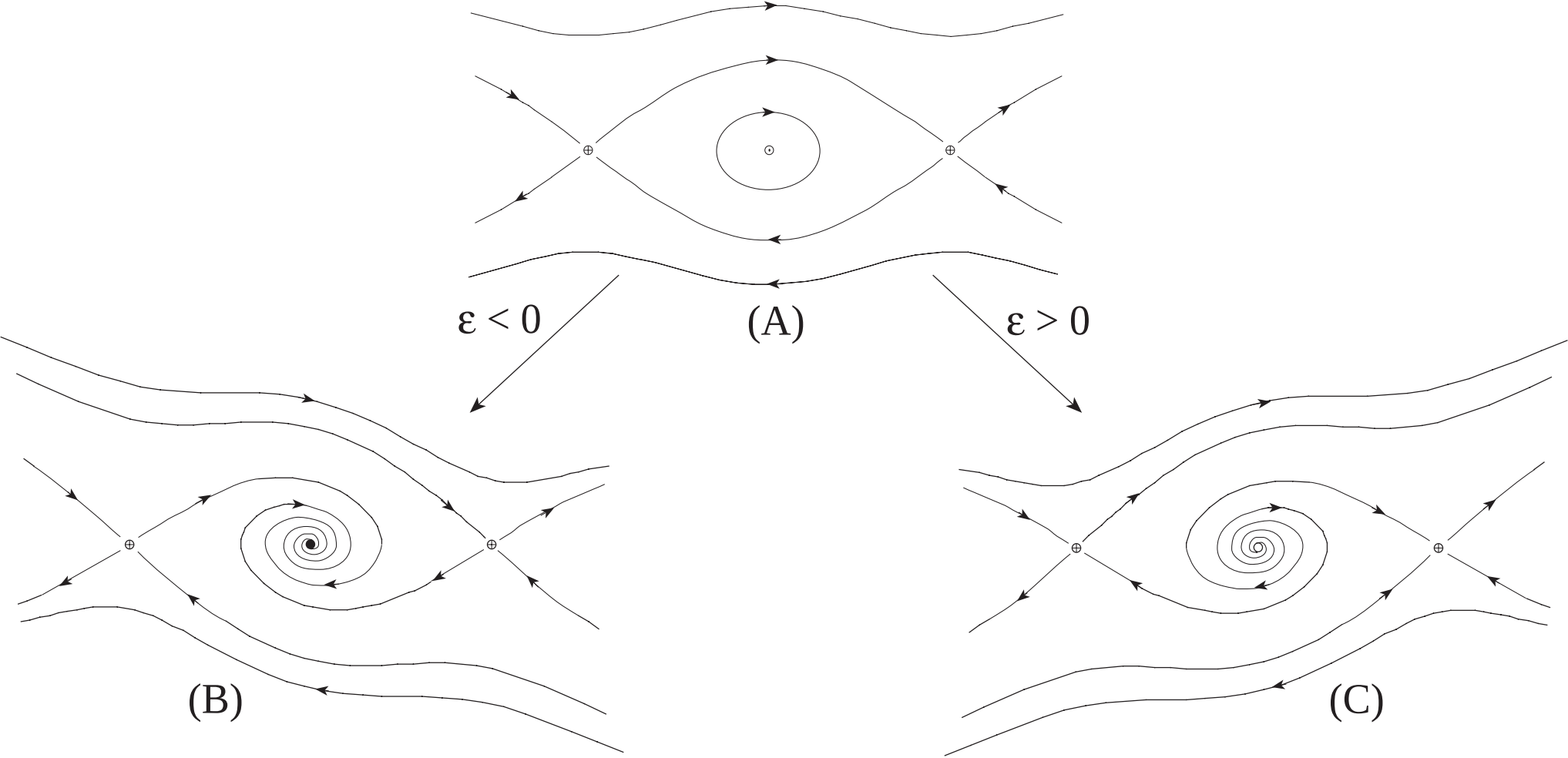
ε < 0
(A)
ε > 0
(B)
(C)

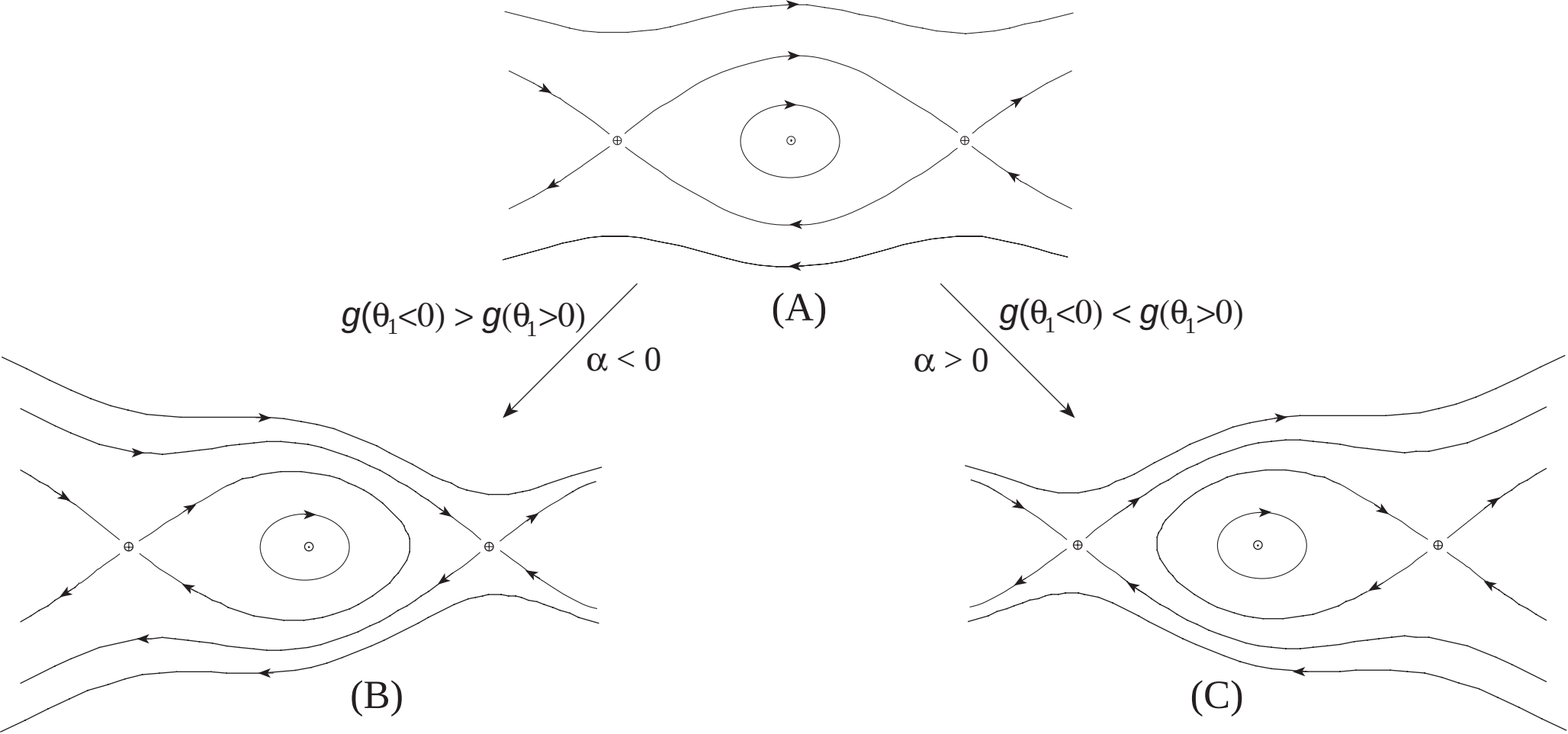
(A)
$g(\theta_1<0) > g(\theta_1>0)$
$\alpha < 0$
$g(\theta_1<0) < g(\theta_1>0)$
$\alpha > 0$
(B)
(C)

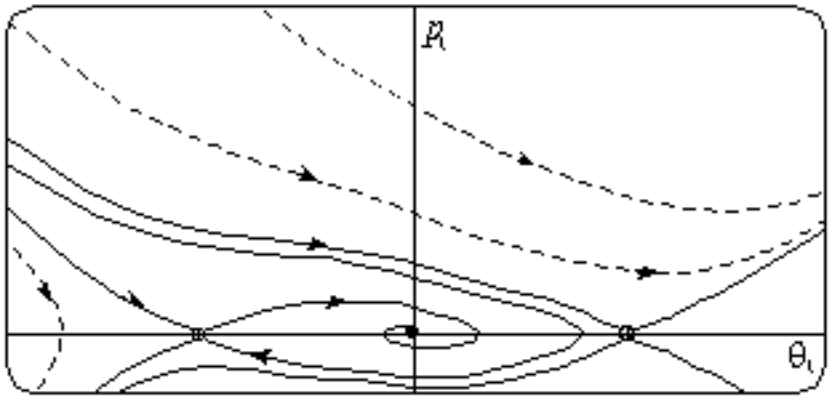

(A)

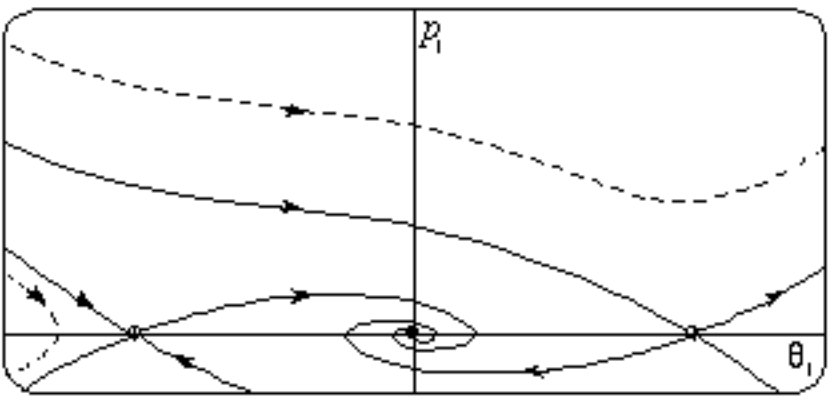

(B)

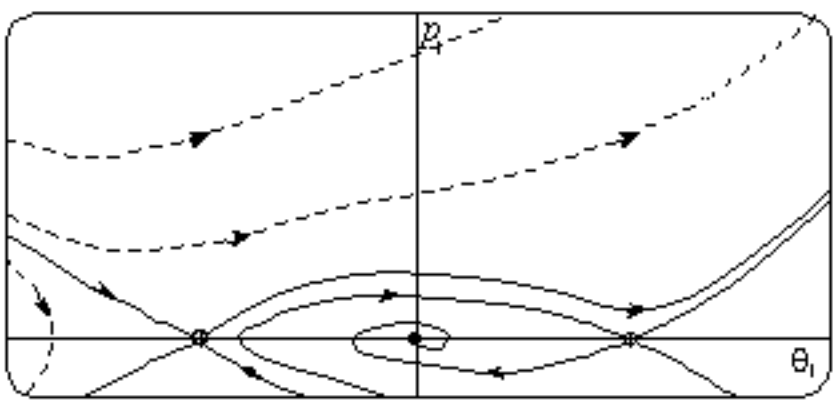

(C)

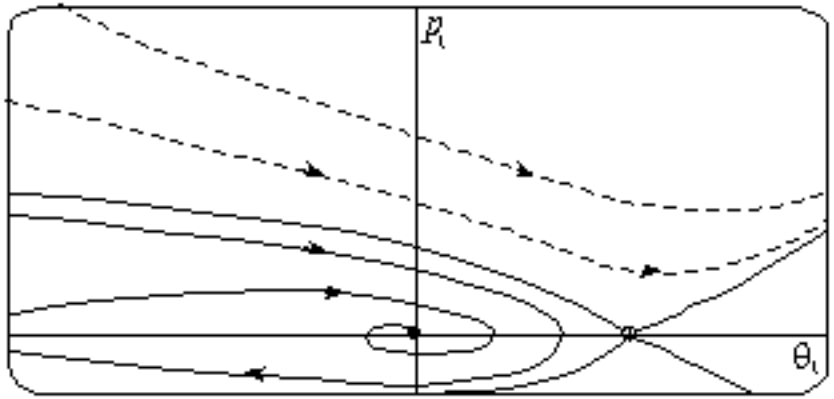

(D)

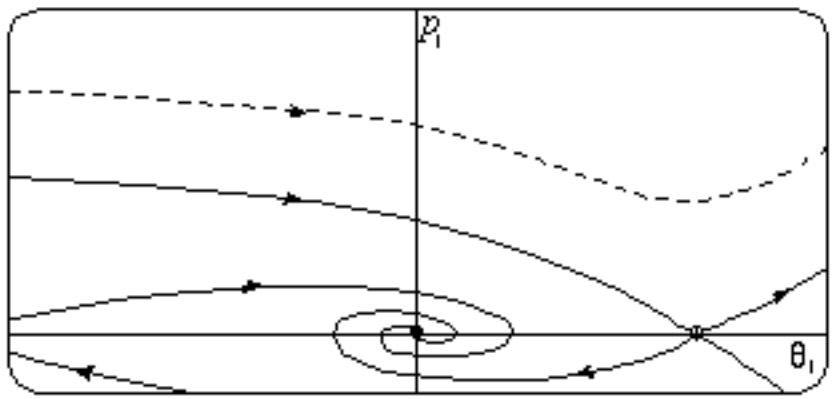

(E)

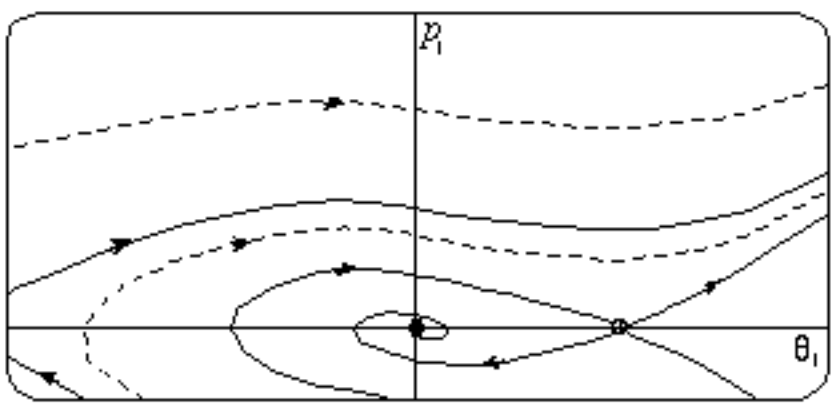

(F)

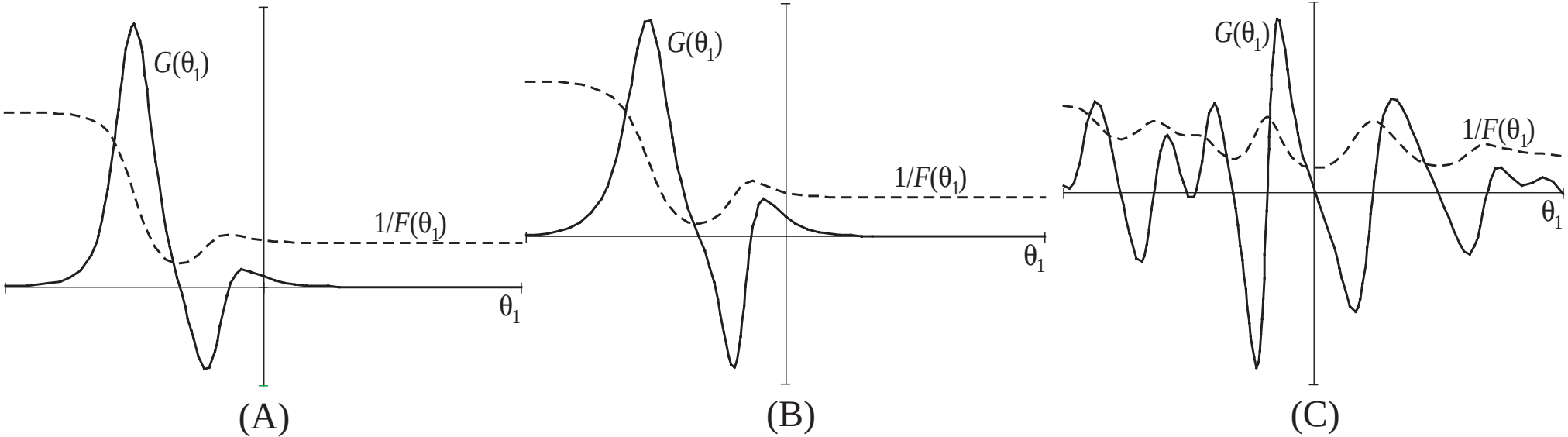
G(θ1)
1/F(θ1)
θ1
(A)
G(θ1)
1/F(θ1)
θ1
(B)
G(θ1)
1/F(θ1)
θ1
(C)